

# Control analysis of an electropneumatic actuator with full convection model: toward minimum energy actuation

Mouchira Abidi, Eric Bideaux, Xavier Brun, Sylvie Sesmat

► **To cite this version:**

Mouchira Abidi, Eric Bideaux, Xavier Brun, Sylvie Sesmat. Control analysis of an electropneumatic actuator with full convection model: toward minimum energy actuation. JFPS, Oct 2011, Okinawa, Japan. pp.2A2-4. hal-00814316

**HAL Id: hal-00814316**

**<https://hal.archives-ouvertes.fr/hal-00814316>**

Submitted on 30 Apr 2019

**HAL** is a multi-disciplinary open access archive for the deposit and dissemination of scientific research documents, whether they are published or not. The documents may come from teaching and research institutions in France or abroad, or from public or private research centers.

L'archive ouverte pluridisciplinaire **HAL**, est destinée au dépôt et à la diffusion de documents scientifiques de niveau recherche, publiés ou non, émanant des établissements d'enseignement et de recherche français ou étrangers, des laboratoires publics ou privés.

# CONTROL ANALYSIS OF AN ELECTROPNEUMATIC ACTUATOR WITH FULL CONVECTION MODEL: TOWARD MINIMUM ENERGY ACTUATION

Mouchira ABIDI\*, Eric BIDEAUX\*, Xavier BRUN\*, and Sylvie SESMAT\*

Ampère Lab, UMR CNRS 5005, INSA Lyon,  
University of Lyon  
25 avenue Jean Capelle, Villeurbanne, F-69621, FRANCE  
(E-mail: [eric.bideaux@insa-lyon.fr](mailto:eric.bideaux@insa-lyon.fr))

## ABSTRACT

Today it is no more reasonable to think that air is free. In order to increase energy efficiency, the control of electropneumatic actuator requires the energy balance in terms of air flow delivered by the power modulators to be optimized during tasks such as trajectory tracking. This paper tries to tackle two essential difficulties when dealing with pneumatic actuation. First, the modeling of the heat transfer phenomena in the cylinder chambers and second, control syntheses taking into account a realistic representation of the temperature dynamic. As a consequence, this approach enables to address properly the optimization of the overall actuation efficiency.

## KEY WORDS

Electropneumatic, heat transfer, model analysis, linear control

## NOMENCLATURE

$h$	specific enthalpy (J/kg)	$c_v$	specific heat capacity at constant volume (J/kg/K)
$m$	mass of gas (kg)	$c_p$	specific heat capacity at constant pressure (J/kg/K)
$U$	internal energy (J)	$r$	perfect gas constant per mass unit (J/kg/K)
$\frac{dQ}{dt}$	heat exchange (J/s)	$\gamma$	adiabatic index
$P$	pressure (Pa)	$k$	polytropic constant
$T$	temperature (K)	$k_{air}$	air thermal conductivity (J/s/K/m)
$q_m$	mass flow rate (kg/s)	$\mu$	air dynamic viscosity (Ns/m <sup>2</sup> )
$u$	servo-distributor input voltage (V)	$g$	gravity acceleration (m/s <sup>2</sup> )
$y$	piston position (m)	$b$	viscous coefficient (N/m/s)
$v$	piston velocity (m/s)	$M$	moving load (kg)
$V$	chamber volume (m <sup>3</sup> )	$S$	area of the piston (m <sup>2</sup> )
$F$	force (N)	$A$	heat exchange area (m <sup>2</sup> )
		$\lambda$	heat exchange coefficient (J/K/m <sup>2</sup> )
		$t$	time (s)
		$\underline{x}$	state vector
		$\delta$	variation

### Subscripts and superscripts

0	external or wall
ext	external
N	chamber N
P	chamber P
S	supply pressure
E	exhaust pressure
e	equilibrium
f	friction

## INTRODUCTION

For pneumatic applications, the overall energy balance must be made in terms of power consumption of the compressor supplying the fluid. In hydraulic and electric applications, energy consumption can easily be evaluated but, when dealing with compressible fluids [1, 2, 3], the energy is related to mass flow rate [4] but also to temperature [5, 6]. However, temperature measurement is still a bottleneck in terms of time constant in regard with the dynamic of the actuation and the modeling of heat transfer behavior is usually drastically simplified.

Recent works on modeling heat transfer in reservoir have resulted in simulation models with detailed convection phenomena according to air flow behavior [6, 7]. These models have been validated experimentally in different configurations and air flow conditions. One of the main interests of these results is that the real energy consumption can now be evaluated on line and in real time using state observers based on cheap and large bandwidth measurement equipments as pressure sensors.

The aim of this work is to explore the interest of temperature dynamic in the synthesis of the control law in order to tackle different drawbacks of electropneumatic actuation such as stick-slip [9] and energy efficiency. Consequently, a model with full heat transfer phenomena and temperature dynamic is proposed. Then, this model is used to perform the synthesis of linear laws taking into account these phenomena.

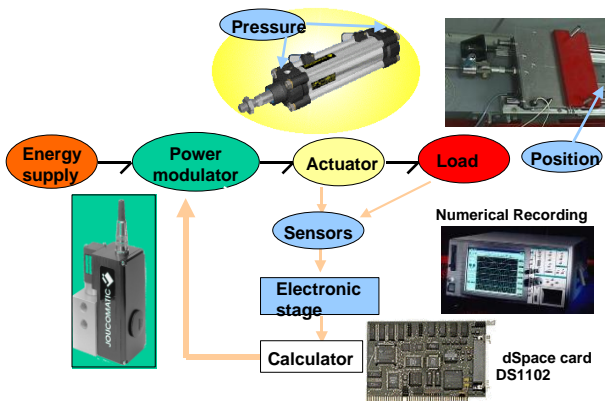


Figure 1: Experimental rig

The first section is dedicated to the modeling of the system where a model taking into account a full convection model for air in the cylinder is proposed. Then the next sections focus on the comparison of two modeling approaches: the first model is based on the classical polytropic hypothesis, whereas the second model takes into account heat exchanges. The first step consists in the comparison of the open-loop dynamic of the linearized models according to piston position. A state feedback control is then designed for each model. This enables the comparison of the system behavior according to the model used for the control synthesis. In this last part, a virtual prototype of the actuator is used and the results are discussed in terms of temperature evolution and energetic performances.

## SYSTEM MODELING

The experimental bench (Fig. 1 and 2) is an in-line electropneumatic servodrive controlled by two three-way servo-distributors.

### Mechanical part:

The stroke length is half a meter and the total moving length is 17 kg. The electropneumatic system model uses classical assumptions [10]: by considering the pressure behavior in a chamber with variable volume and the mechanical equation which includes pressure force, viscous friction and dry friction ( $F_f$ ) and an external force ( $F_{ext}$ ) due to atmospheric pressure.

$$\begin{cases} M \frac{dv}{dt} = S_P P_P - S_N P_N - F_{ext} - F_f \\ \frac{dy}{dt} = v \end{cases} \quad (1)$$

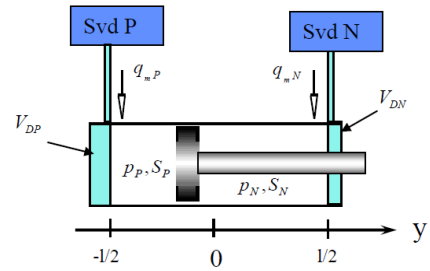


Figure 2: Scheme and notation

Using the theory of multi-scale systems, the dynamics of the servo-valves can be neglected [9]. Then the model can be reduced to a static characteristic for given supply and exhaust pressures and is described by two relationships  $q_{mP}(P_P, u_P)$  and  $q_{mN}(P_N, u_N)$  between the mass flow rates  $q_{mP}$  and  $q_{mN}$ , the input voltages  $u_P$  and  $u_N$ , and the output pressures  $P_P$  and  $P_N$ .

The following assumptions are taken into account for establishing the thermodynamic model:

- air is a perfect gas,
- pressure and temperature are homogenous in the chambers,
- kinetic and gravitational energy of the fluid, as well as viscous work and cylinder flow leakages are considered as negligible.

The thermodynamic model obtained by applying the thermodynamic principles and mass conservation is defined as follow:

#### Chamber N:

$$\begin{cases} \frac{dU_N}{dt} = q_{mSN}h_S - q_{mNE}h - P_N \frac{dV_N}{dt} + \frac{dQ_N}{dt} \\ \frac{dm_N}{dt} = q_{mSN} - q_{mNE} \\ \frac{dV_N}{dt} = -S_N v \end{cases} \quad (2)$$

$$\text{and } \begin{cases} P_N = \frac{r}{c_v} \frac{U_N}{V_N} \\ T_N = \frac{1}{c_v} \frac{U_N}{m_N} \end{cases} \quad (3)$$

#### Chamber P:

$$\begin{cases} \frac{dU_P}{dt} = q_{mSP}h_P - q_{mPE}h - P_P \frac{dV_P}{dt} + \frac{dQ_P}{dt} \\ \frac{dm_P}{dt} = q_{mSP} - q_{mPE} \\ \frac{dV_P}{dt} = S_P v \end{cases} \quad (4)$$

$$\text{and } \begin{cases} P_P = \frac{r}{c_v} \frac{U_P}{V_P} \\ T_P = \frac{1}{c_v} \frac{U_P}{m_P} \end{cases} \quad (5)$$

#### Thermal Exchange:

The thermal exchange from the gas in each chamber and the cylinder is developed. The proposed macroscopic model is based on the dimensional analysis theory and takes into account free-forced convection phenomena as well as wall thermal conduction. The model gives the equivalent macroscopic temperature in a chamber according to chamber state, flow conditions, and external temperature. It has been validated experimentally for charge and discharge tests, which justify the proposed estimation.

$$\frac{dQ_N}{dt} = \lambda(T_N, P_N) \cdot A_N(y) \cdot (T_0 - T_N) \quad (6)$$

$$\frac{dQ_P}{dt} = \lambda(T_P, P_P) \cdot A_P(y) \cdot (T_0 - T_P) \quad (7)$$

where  $A(y)$  is the heat exchange area between gas and walls according to the piston position, and  $\lambda(T, P)$  is the heat transfer coefficient obtained using the dimensionless number listed below :

- Nusselt number,  $Nu = \frac{\lambda D}{k_{air}} = \xi \cdot Gr^\beta \cdot Pr^{\beta'}$
- Grashof number,  $Gr = \frac{gD^3(T_0 - T)P^2}{r^2 \mu^2 T^3}$
- Prandtl number,  $Pr = \frac{c_p \mu}{k_{air}}$

In this relations,  $\beta$  and  $\beta'$  are coefficient experimentally determined and  $D$  is a characteristic length for the convection phenomena.

In the pressure and temperature range for this application, the Prandtl number for the gas can be considered as constant. Then, the heat transfer coefficient can be expressed for each chamber as:

$$\begin{aligned} \lambda(T_{P(\text{or}N)}, P_{P(\text{or}N)}) &= \lambda_{P(\text{or}N)} \\ &= \xi \frac{k}{D} \left[ \frac{gD^3(T_{cyl} - T_{P(\text{or}N)})P_{P(\text{or}N)}^2}{r^2 \mu^2 T_{P(\text{or}N)}^3} \right]^\beta \end{aligned} \quad (8)$$

Using (3) and (5) enables the substitution in (2) and (4) of the natural state variables (internal energy and mass) by pressure and temperature in each chamber. The obtained model has 6 state variables and is given by the following equations:

$$\begin{cases} \frac{dy}{dt} = v \\ \frac{dv}{dt} = \frac{1}{M} (S_P P_P - S_N P_N - F_{ext} - F_f) \\ \frac{dP_N}{dt} = \frac{\gamma T_N}{V_N(y)} (q_{mSN} - q_{mNE}) - \frac{\gamma(T_N - T_0)}{V_N(y)} q_{mSN} \\ \quad + \frac{\gamma S_N P_N}{V_N(y)} v + (\gamma - 1) \frac{A_N(y) \lambda_N}{V_N(y)} (T_0 - T_N) \\ \frac{dP_P}{dt} = \frac{\gamma T_P}{V_P(y)} (q_{mSP} - q_{mPE}) - \frac{\gamma(T_P - T_0)}{V_P(y)} q_{mSP} \\ \quad - \frac{\gamma S_P P_P}{V_P(y)} v + (\gamma - 1) \frac{A_P(y) \lambda_P}{V_P(y)} (T_0 - T_P) \\ \frac{dT_N}{dt} = \frac{(\gamma - 1) T_N}{P_N V_N(y)} \left[ \left( \gamma \frac{T_0}{T_N} - 1 \right) c_v T_N q_{mSN} \right. \\ \quad \left. - (\gamma - 1) c_v T_N q_{mNE} + P_N S_N v + \lambda_N A_N(y) \cdot (T_0 - T_N) \right] \\ \frac{dT_P}{dt} = \frac{(\gamma - 1) T_P}{P_P V_P(y)} \left[ \left( \gamma \frac{T_0}{T_P} - 1 \right) c_v T_P q_{mSP} \right. \\ \quad \left. - (\gamma - 1) c_v T_P q_{mPE} - P_P S_P v + \lambda_P A_P(y) \cdot (T_0 - T_P) \right] \end{cases} \quad (9)$$

## EQUILIBRIUM SET AND LINEARIZED MODEL

The previous physical model of the electropneumatic system is too complex for an analytic approach. A linearized model has to be established first for analyzing the modal characteristic of the model, and second for the synthesis of a state feedback control law. Let us assume that:

- the heat transfer coefficient is nearly constant at equilibrium,
- the mass flow rate characteristic of the servovalve is not depending on the temperature and is given by:

$$\begin{cases} q_{mN}(P_N, u) = -q_{mSN}(P_S, T_S, P_N, u) + q_{mNE}(P_N, T_N, P_E, u) \\ q_{mP}(P_P, u) = q_{mSP}(P_S, P_P, T_S, u) - q_{mPE}(P_P, T_P, P_E, u) \end{cases} \quad (6)$$

For a single input non-linear model  $\dot{x} = f(x, u)$ , the equilibrium set is defined by  $E = \{(x_e, u_e) \in \mathcal{R}^n \times \mathcal{R} / f(x_e, u_e) = 0\}$ . In our case the equilibrium set can be deduced from (9):

$$\begin{cases} y^e \\ v^e = 0 \\ T_N^e = T_P^e = T_0 \\ q_{mN}(P_N^e, -u^e) = 0 \\ q_{mP}(P_P^e, u^e) = 0 \\ S_P P_P^e - S_N P_N^e - F_{ext}^e = 0 \end{cases} \quad (10)$$

$$\frac{d}{dt} \begin{bmatrix} \delta y \\ \delta v \\ \delta P_N \\ \delta P_P \\ \delta T_N \\ \delta T_P \end{bmatrix} = \underbrace{\begin{bmatrix} 0 & 1 & 0 & 0 \\ 0 & -\frac{b}{M} & -\frac{S_N}{M} & \frac{S_P}{M} \\ 0 & \frac{\gamma S_N P_N^e}{V_N(y^e)} & -\frac{\gamma T_N^e}{V_N(y^e)} C_{P_N, N}^e & 0 \\ 0 & -\frac{\gamma S_P P_P^e}{V_P(y^e)} & 0 & -\frac{\gamma T_P^e}{V_P(y^e)} C_{P_P, P}^e \\ 0 & \frac{(\gamma-1) S_N T_N^e}{V_N(y^e)} & -\frac{(\gamma-1) r T_N^e}{P_N^e V_N(y^e)} C_{P_N, N}^e & 0 \\ 0 & -\frac{(\gamma-1) S_P T_P^e}{V_P(y^e)} & 0 & -\frac{(\gamma-1) r T_P^e}{P_P^e V_P(y^e)} C_{P_P, P}^e \end{bmatrix}}_{A_{heat}} \begin{bmatrix} \delta y \\ \delta v \\ \delta P_N \\ \delta P_P \\ \delta T_N \\ \delta T_P \end{bmatrix} + \underbrace{\begin{bmatrix} 0 & 0 \\ 0 & 0 \\ -\frac{(\gamma-1) A_N^e \lambda_N^e}{V_N(y^e)} & 0 \\ 0 & -\frac{(\gamma-1) A_P^e \lambda_P^e}{V_P(y^e)} \\ -\frac{(\gamma-1) T_N^e A_N^e \lambda_N^e}{P_N^e V_N(y^e)} & 0 \\ 0 & -\frac{(\gamma-1) T_P^e A_P^e \lambda_P^e}{P_P^e V_P(y^e)} \end{bmatrix}}_{B_{heat}} \delta u \quad (13)$$

$$\frac{d}{dt} \begin{bmatrix} \delta y \\ \delta v \\ \delta P_N \\ \delta P_P \end{bmatrix} = \underbrace{\begin{bmatrix} 0 & 1 & 0 & 0 \\ 0 & -\frac{b}{M} & -\frac{S_N}{M} & \frac{S_P}{M} \\ 0 & \frac{k P_N^e S_N}{V_N(y^e)} & -\frac{1}{\tau_N^e} & 0 \\ 0 & \frac{k P_P^e S_P}{V_P(y^e)} & 0 & -\frac{1}{\tau_P^e} \end{bmatrix}}_{A_{poly}} \begin{bmatrix} \delta y \\ \delta v \\ \delta P_N \\ \delta P_P \end{bmatrix} + \underbrace{\begin{bmatrix} 0 \\ 0 \\ -\frac{k r T_0}{V_N(y^e)} G_{uN}^e \\ \frac{k r T_0}{V_P(y^e)} G_{uP}^e \end{bmatrix}}_{B_{poly}} \delta u \quad (14)$$

## OPEN LOOP STABILITY

In this section a comparative study of both 4<sup>th</sup> and 6<sup>th</sup> order open loop systems is presented. In linear system, poles have influence on stability system response,

The three unknown variables  $(P_P^e, P_N^e, u^e)$  are determined by solving graphically the three last equations in (10) using the mass flow rate characteristic of the servovalve.

Let us note the variations in a neighborhood of the equilibrium set as:

$$\begin{cases} \delta x = x - x^e \\ \delta u = u - u^e \end{cases} \quad (11)$$

The linearized model is then defined by (12) using following notations for the flow characteristics of the servovalve around the equilibrium point:

$$\begin{aligned} G_{uN}^e &= -\left. \frac{\partial q_{mN}(P_N, u)}{\partial u} \right|_{(P_N^e, -u^e)}, C_{P_N, N}^e = \left. \frac{\partial q_{mN}(P_N, u)}{\partial P_N} \right|_{(P_N^e, -u^e)} \\ G_{uP}^e &= \left. \frac{\partial q_{mP}(P_P, u)}{\partial u} \right|_{(P_P^e, u^e)}, C_{P_P, P}^e = -\left. \frac{\partial q_{mP}(P_P, u)}{\partial P_P} \right|_{(P_P^e, u^e)} \\ \tau_P^e &= \frac{V_P(y^e)}{k r T_0 C_{P_P, P}^e}, \tau_N^e = \frac{V_N(y^e)}{k r T_0 C_{P_N, N}^e} \end{aligned} \quad (12)$$

In most of the cases, for control purposes, the thermodynamic transformation of the gas in the cylinder is assumed to be polytropic and heat transfer with walls is neglected. Taking into account those simplifications, it allows the reduction of the model to a 4<sup>th</sup> order model defined by (14). The two models can now be compared analytically according to the formulation shown below.

transient response and bandwidth. For both linearized models (12) and (14), the stability can be analyzed according to the considered equilibrium state (10), which depends on pressures and piston position. Here the polytropic index  $k$  has been set equal to 1.2 in the polytropic model (14); this value is generally the one

used for control purposes as it gives a good approximation of the cylinder dynamic in most of the cases.

Fig. 3 and 4 show respectively the evolution of the poles of the 4<sup>th</sup> and 6<sup>th</sup> order models for different piston positions. Fig. 5 presents a comparison of the dynamic of the poles calculated at middle stroke.

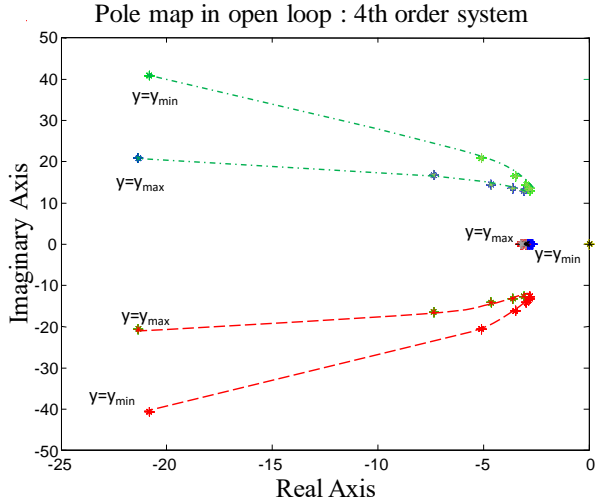


Figure 3: Pole evolution in open loop for the 4<sup>th</sup> order model at different equilibrium position

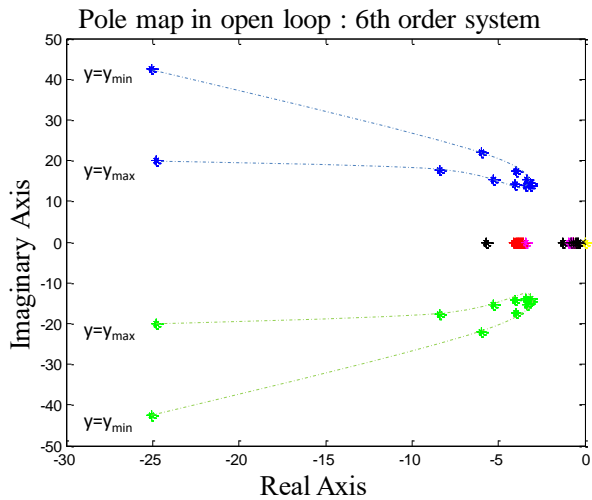


Figure 4: Pole evolution in open loop for the 6<sup>th</sup> order model at different equilibrium position

These two figures show clearly that the piston position plays a crucial role on the system dynamic. We can also remark that poles at  $y_{min}$  and  $y_{max}$  are naturally not identical since the cylinder has a rod on only one side and the chambers are consequently non symmetrical. The influence of the temperature dynamic can clearly be observed with the two new real poles at low frequency, but also because it changes the location of the other poles. These changes are more clearly shown on Fig. 5

where the dynamic of the poles calculated at middle stroke is compared for both models.

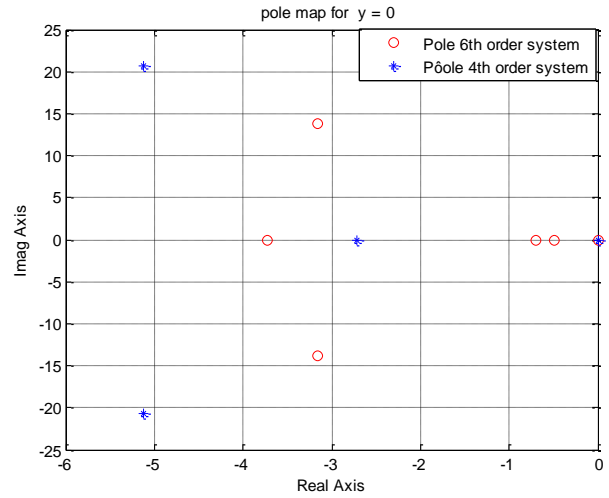


Figure 5: Comparison of the pole in open loop for both models at half-stroke

It can be concluded that classical hypothesis that states that the temperature dynamic can be neglected is not so obvious. All the dynamics are of the same order of magnitude. Nevertheless, the polytropic model with a polytropic index  $k = 1.2$  seems to catch properly the main effects.

In the next section, basic control laws are designed in order to outline the differences between the two approaches (models).

## STATE FEEDBACK CONTROL LAW

The position control of pneumatic actuators has widely been studied and many linear and non linear techniques have been successfully applied [11, 12, 13]. Our goal is not here to design a control law leading to high performances, but rather to consider a linear control approach, such as state feedback, that allows all the information provided by the model to be taken into account, and the system to be studied in the linear domain. Of course, the implementation of such a control law is not considered here, as feedback on all states is not realistic on real systems, especially for temperatures.

In this section, the state feedback control law with pole placement is synthesized in order to reach about the same kind of step response for both linearized models. For the polytropic model, the polytropic index  $k$  is set equal to 1.2, and for the model taking into account the temperature dynamic, the heat exchange coefficient is fixed to 15 J/s/m<sup>2</sup>/K.

The first step in the pole placement approach is to define the pole locations for the closed loop. For high order system, which cannot be approximated by second order systems (it is the case here, especially at half-

stroke), this choice can be complex. The ITAE [14] is one of the techniques that can be applied at the pole selection step. In our case, in order to avoid command saturation, the following closed loop pole locations have been chosen:

Prototype Response Poles: ITAE transfer functions		
order	Pole locations for $w_0=1\text{rad/s}$	
4	$s+0.4240 \pm 1.2630 j$	$w_n = 1.33 \text{ rad/s}, \zeta = 0.32$
	$s+0.6260 \pm 0.4141 j$	$w_n = 0.75 \text{ rad/s}, \zeta = 0.83$
6	$s+0.3099 \pm 1.2634 j$	$w_n = 1.30 \text{ rad/s}, \zeta = 0.24$
	$s+0.5805 \pm 0.7828 j$	$w_n = 0.97 \text{ rad/s}, \zeta = 0.59$
	$s+0.7346 \pm 0.2873 j$	$w_n = 0.79 \text{ rad/s}, \zeta = 0.93$

By substituting  $s$  by  $s/w_0$ , pole location can be obtained for any values of  $w_0$ , the open-loop natural frequency.

From the state feedback control defined as  $\delta u = -K \cdot \delta x$ , the chosen closed loop poles are also the eigenvalues of the closed loop state matrix  $(A - BK)$ . This leads to the following feedback gain matrix  $K$  for both models at half-stroke.

order	Feedback gain matrix (K)
4	$[0.9637 \quad -1.5072 \quad 0 \quad 0]$
6	$[29.6804 \quad -17.7596 \quad -0.0001 \dots$ $\dots 0.0022 \quad -10.5847 \quad 1.2379]$

The state feedback gains can also be calculated for different piston positions. Fig. 4 and 5 show the pole evolution in closed loop for the 4<sup>th</sup> and 6<sup>th</sup> order models with the choice made for each model.

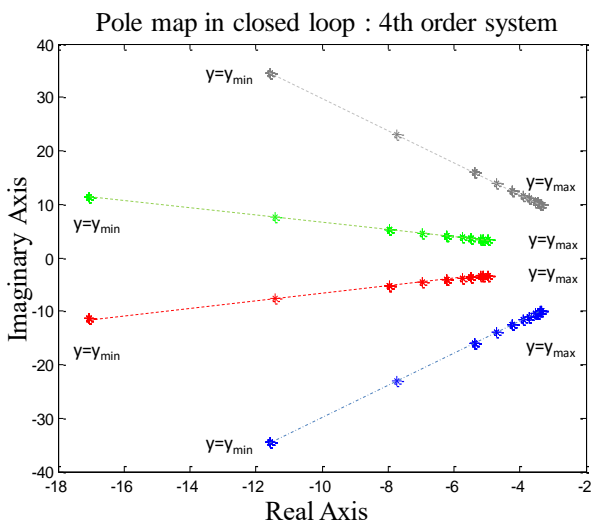


Figure 6: Pole evolution in closed loop for the 4<sup>th</sup> order model at different equilibrium position

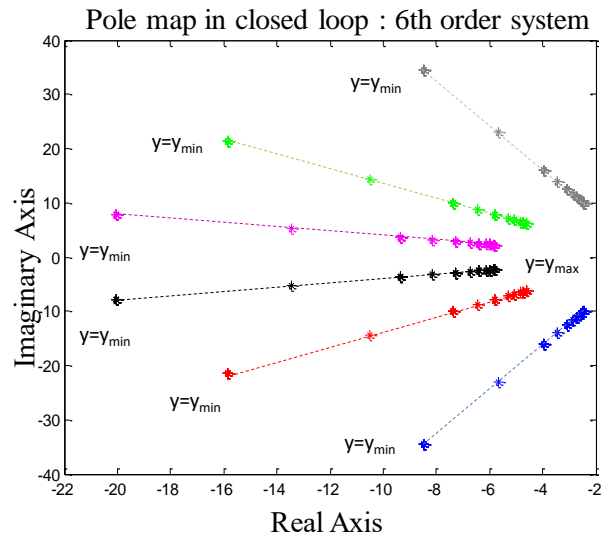


Figure 7: Pole evolution in closed loop for the 6<sup>th</sup> order model at different equilibrium position

A completer ....

### SIMULATION

In order to compare the two synthesized control laws, a simulation model of the actuator has been implemented in the LMS Imagine.Lab AMESim (Fig. 8). This model takes into account several phenomena, which have been neglected at the control design step:

- the heat transfer coefficient is variable according to (8),
- dry friction with Stribeck effects is considered: stiction force is equal to 50 N, and Coulomb friction force is equal to 30 N,
- leakages between chambers are taken into account,
- the dynamic and the real flow characteristics [15] of the servovalves are fully modeled.

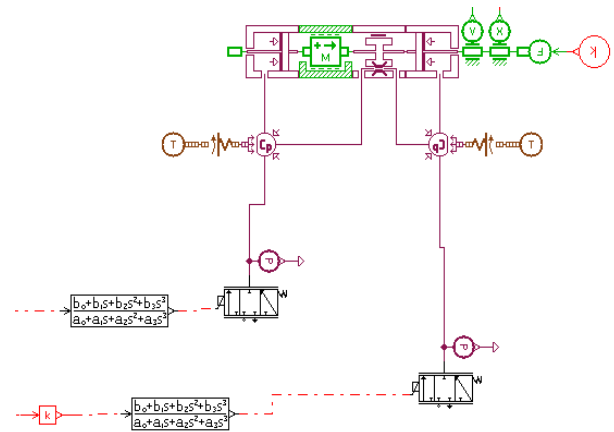


Figure 8: AMESim model

The feedback gain matrix calculated for half-stroke is used for step responses around this position. Fig. 9 shows the position of the piston in both cases.

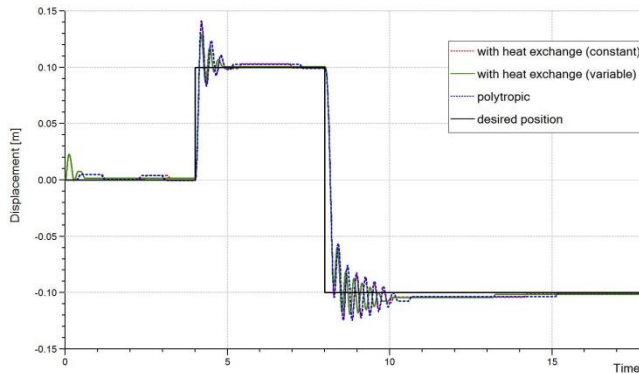


Figure 9: Comparison of the piston displacement for step inputs with the same control law

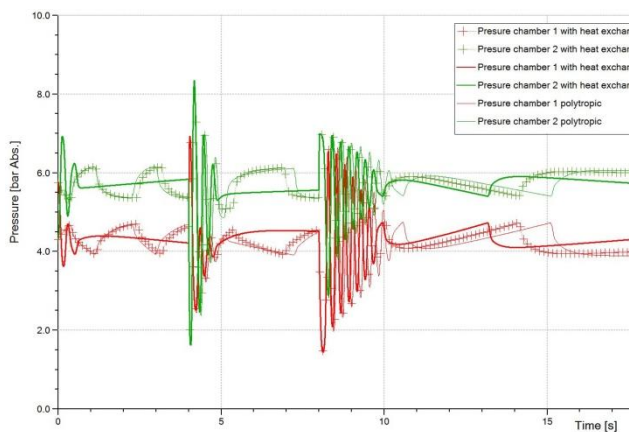


Figure 10: Comparison of the pressures in the cylinder chambers

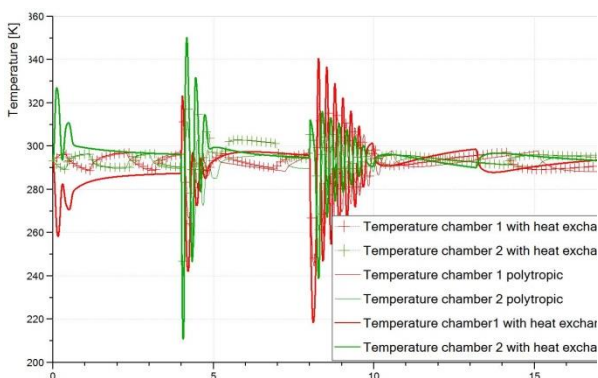


Figure 11: Comparison of the temperatures in the cylinder chambers

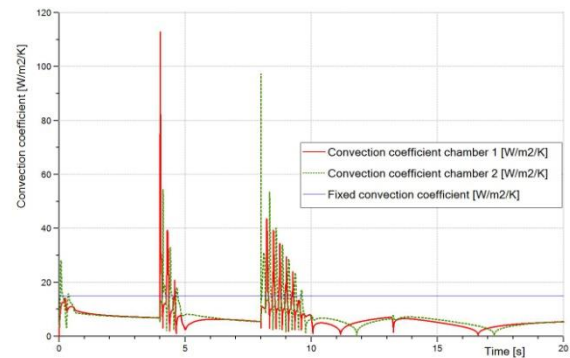


Figure 11: Evolution of the heat transfer coefficient in the cylinder chambers

## CONCLUSION

In this paper, we have shown that it could be worth to take into account the temperature dynamic for the design of the control law. First, the influence of temperature dynamic is significant; second, it leads to a better control of the system. The simulations have shown that neither the polytropic approach, neither a model with a constant heat exchange coefficient can properly represent the temperature magnitude or dynamic.

This type of approach allows now the energy efficiency problem to be studied in details. Further works should now revisit energy efficient control law, which have already been discussed in previous work [16]; thermal share could be an answer to the minimization of energy. On the proposed model basis, the adequate path planning can be developed and the choice of the structure of the system can also be questioned, for example in terms of energy recovery. This development will however require more advanced control strategy, such as flatness theory or backstepping control techniques [17, 18].

## REFERENCES

- [1] B.W. Andersen, "The analysis and design of pneumatic systems", New-York: John Wiley and Sons, 1967, 302p.
- [2] D. Mc Cloy D. and H.R. Martin, "Control of Fluid Power: Analysis and Design", Chichester (England), Ellis Horwood, 1980. 510p.
- [3] L.A. Zalmanzon, "Components for pneumatic control instruments", Oxford: Pergamon press, 1965, 320 p.
- [4] International Standard ISO 6358, "Pneumatic Fluid Power Components using Compressible Fluids – Determination of Flow-rate Characteristics", 1989. 15p.



- [5] T. Kagawa, K. Kawashima, and T. Fujita, "Effective area measurement method using isothermal chamber", *Hydraulics and Pneumatics*, Vol. 26(1), pp. 76–78, 1995.
- [6] K. Kawashima, T. Kagawa, and T. Fujita, "Instantaneous flow rate measurement of ideal gases", *Journal of Dynamic Systems, Measurement and Control*, vol. 1222:174–178, march 2000.
- [7] R. de Giorgi, E. Eric Bideaux, and S. Sesmat, "Using inverse models for determining orifices mass flow rate characteristics", 6th JFPS Japan International Symposium on Fluid Power, Tsukuba, Japan, November 7-10, 2005.
- [8] R. De Giorgi, E. Bideaux, S. Sesmat Dynamic thermal model of a discharging process of a pneumatic chamber, 4th FPNI PHD Symposium, Sarasota, 2006.
- [9] Study of "Sticking and restarting phenomenon" in electropneumatic positioning systems, Brun X., Sesmat S., Thomasset D., Scavarda S., *Journal of Dynamic Systems Measurement and Control*, Transaction of the ASME 127, 1, pp. 173-184, 2005.
- [10] Shearer, J.L., "Study of pneumatic processes in the continuous control of motion with compressed air. Parts I and II", *Trans. Am. Soc. Mech. Eng.*, 78, 233-249, 1956.
- [11] Bachmann, J.R., Surgenor, B.W., "On design and performance of a closed circuit pneumatic positioning system", fifth Scandinavian International Conf. on Fluid Power, Linköping, Sweden, Vol.1, pp 309-322, May 28-30, 1997.
- [12] Richard, E., Scavarda, S., "Comparison between Linear and Nonlinear control of an electropneumatic servodrive", *Jour. of Dyn. Syst. Meas. & Control*, June 1996, Vol. 118, p 245-252.
- [13] Brun X., Belgharbi M., Sesmat S., Thomasset D., Scavarda S., "Control of an electropneumatic actuator, comparison between some linear and nonlinear control laws", *Jour. of Syst. and Control Engineering*, 1999, Vol. 213, N°15, p 387-406.
- [14] G. F. Franklein, J.D. Powell, A. Emami-Naeini, "Feedback control of dynamic systems", Prentice Hall; 4 edition, January 15, 2002.
- [15] Belgharbi, M., Thomasset, D., Scavarda, S., & Sesmat, S. "Analytical model of the flow stage of a pneumatic servo-distributor for simulation and nonlinear control", 6th Scandina. Int. Conf. on Fluid Power, SICFP'99, pp. 847-860, 1999, Tampere, Finland.
- [16] Brun, X., Thomasset, D., Sesmat, & S., Scavarda, S., "Limited energy consumption in positioning control of electropneumatic actuator", Bath Workshop on Power Transmission & Motion Control, 1999, pp 199-211, Bath, England.
- [17] Isidori, A., "Nonlinear control systems", New York: Springer Verlag, 2nd edition, 479 p., 1989.
- [18] M. Smaoui, X. Brun, D. Thomasset, "A study on tracking position control of an electropneumatic system using backstepping design", *Control Engineering Practice*, Vol. 14, Issue 8, August 2006, Pages 923-933.